High Energy Neutrinos from the Fermi Bubbles

Cecilia Lunardini and Soebur Razzaque

High Energy Neutrinos from the Fermi Bubbles

Cecilia Lunardini[1, 2, *] and Soebur Razzaque[3, 4, †]

[1]*Arizona State University, Tempe, AZ 85287-1504*
[2]*RIKEN BNL Research Center, Brookhaven National Laboratory, Upton, NY 11973*
[3] *School of Physics, Astronomy and Computational Sciences, George Mason University, Fairfax, VA 22030*
[4] *Resident at the Space Science Division, US Naval Research Laboratory, Washington, DC 20375*

Recently the *Fermi*-LAT data have revealed two gamma-ray emitting bubble-shaped structures at the Galactic center. If the observed gamma rays have hadronic origin (collisions of accelerated protons), the bubbles must emit high energy neutrinos as well. This new, Galactic, neutrino flux should trace the gamma ray emission in spectrum and spatial extent. Its highest energy part, above 20–50 TeV, is observable at a kilometer scale detector in the northern hemisphere, such as the planned KM3NeT, while interesting constraints on it could be obtained by the IceCube Neutrino Observatory at the South pole. The detection or exclusion of neutrinos from the *Fermi* bubbles will discriminate between hadronic and leptonic models, thus bringing unique information on the still mysterious origin of these objects and on the time scale of their formation.

Gamma-ray data in the 1–100 GeV range from the *Fermi*-LAT [1] show a new, unexpected, feature of our galaxy: two huge spheroidal structures (*Fermi* "bubbles", FB from here on), extending up to $\sim 8-9$ kpc ($50°$) out of the galactic center on either side of the galactic disk [2, 3]. Intriguingly, the bubbles coincide spatially with the WMAP "haze" in microwave [4] and the thermal X-ray emission seen by ROSAT [5]. The origins of these three phenomena, and whether they are related, are matters of intense debate [2, 3, 6–9].

If we limit ourselves to the Standard Model of particle physics, there are two main models for the FB. One is the leptonic origin: Compton scattering of relativistic electrons on photons (microwave, or optical/ultraviolet), where the electrons originate from shocks in the outflow of the Galactic center black hole, Sgr A* [3, 8], or from an episodic activity of Sgr A* due to the capture of a star [9] or to a localized star formation (SF) event [10]. The second scenario is the hadronic origin: collision of accelerated protons on background protons in the bubble gas [7]. The collisions produce π^0 mesons, which then decay as $\pi^0 \to \gamma\gamma$. Here the accelerated protons originate in the supernova remnants (SNRs) near the Galactic center. The two scenarios differ widely in the cooling times of the accelerated particles, and therefore in the predicted age of the bubbles: millions of years for the leptonic model, versus billions for the hadronic case. Thus, the origin of the FB will teach us about the time scale of Sgr A*'s activity and about the Galactic star-formation history.

A major signature of the hadronic models – and therefore a discriminator between the leptonic and hadronic models of the FB [7, 11] – is the presence of a high energy, $\sim$ 1–10 TeV neutrino (ν) counterpart of the γ rays (see, e.g., [12]). Indeed, pp collisions produce charged pions, $\pi^{\pm}$, as efficiently as π^0, and muon and electron neutrinos (ν_μ, ν_e) are then produced by decay, e.g., $\pi^+ \to \mu^+ + \nu_\mu \to \nu_\mu + e^+ + \nu_e + \bar{\nu}_\mu$. This mechanism

is also the origin of the observed flux of neutrinos from cosmic-ray interactions in the Earth's atmosphere.

In this Letter we present the first study of neutrinos from the FB, in the hadronic model, and show that they are detectable at a kilometer scale experiment, like the existing IceCube [13], or the planned KM3NeT [14], depending on the detector's location. This is a new signal, whose detection or exclusion will contribute to understanding the physics of the bubbles.
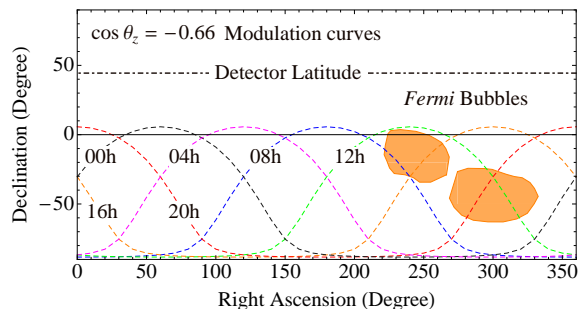

FIG. 1: The contour of the *Fermi* bubbles in equatorial coordinates (shaded), adapted from [3]. Considering θ_z as the zenith angle with respect to a neutrino telescope at a latitude $+43°$ (KM3NeT), the area below each curve has $\cos\theta_z < -0.66$ at a given time of the day (labels on curves).

Figure 1 shows a sketch of the FB in equatorial coordinates. They face the Earth's southern hemisphere, extending to $\sim 60°$ below the equator, and subtend a solid angle $\Omega_b = 0.808$ sr [3]. The bubbles are uniformly bright in γ rays, with sharp edges and a hard spectrum, $dN_\gamma/dE \propto E^{-2}$ [3].

In the hadronic model of Crocker and Aharonian (CA) [7], the bubbles are powered by SNRs, which are widely believed to be the factories of cosmic rays up to 10^{15}–10^{17} eV [17]. The low-density bubble interiors (average density $\langle n_H \rangle \sim 10^{-2}$ cm^{-3} [3]) are created by

prolonged SF activity near the Galactic center, which forms a high-velocity bipolar wind. This wind carries the cosmic ray protons produced in the SNRs to fill the bubble cavities. The interactions of these protons with the diluted hot gas produce the FB as observed by the *Fermi*-LAT. The associated time scale for proton cooling is $\sim 5 \times 10^9$ yr [7], and therefore a SF period of at least this duration is required in the CA model.

To calculate the γ and ν fluxes from pp interactions in the FB we use an injected proton spectrum in the bubble cavities, at steady-state, of the form

$$N_p(E) = N_0 E^{-k} \exp(-E/E_0), \qquad (1)$$

where N_0, k and E_0 are the normalization factor, spectral index and cutoff energy respectively. The cutoff energy, $E_0 \sim 1 - 10$ PeV, is motivated by cosmic-ray acceleration in SNRs [17], and $k \sim 2$ is expected in a Fermi acceleration mechanism. The index of the injected protons remains hard, in the FB, due to a saturation condition realized when the acceleration (in the SNRs) time, pp energy loss (in the FB) time and escape (from the FB) time satisfy a relation: $t_{acc} < t_{loss} \lesssim t_{esc}$ [7]. Using a parameterization from the Monte Carlo code SIBYLL [18], we obtain the fluxes of gamma rays and neutrinos from π^0, $\pi^\pm$ decay, above $\gtrsim 10$ GeV. At lower energies, the fluxes can be modeled with a delta-function approximation. For example, the γ flux is given by

$$\Phi_\gamma(E_\gamma) = \frac{\varphi \langle n_H \rangle}{4\pi D^2 K_\pi} \int_{E_{\pi,th}}^{\infty} dE_\pi \, \frac{\sigma_{pp}(E_c)}{\sqrt{E_\pi^2 - m_\pi^2}} N_p(E_c). \quad (2)$$

Here D is the distance to the bubbles, $K_\pi \approx 0.17$ is the mean fraction of proton kinetic energy converting to π^0, $E_{\pi,th} = E_\gamma + m_\pi^2/4E_\gamma$ is the threshold pion energy, σ_{pp} is the inelastic pp cross section, and $E_c = E_\pi/K_\pi + m_p$. The parameter $\varphi \sim \mathcal{O}(1)$, and is adjusted to match the $E \gtrsim 10$ GeV Monte Carlo results. Note that there is a $\sim 10\%$ uncertainty in the hadronic models [18]. We also neglected a contribution of $\sim 10\%$ or less (depending on the unknown magnetic field in the FB) due to Compton-scattered photons off secondary $e^\pm$. Our calculation gives the fluxes of γ and of $\nu_\mu, \bar{\nu}_\mu, \nu_e, \bar{\nu}_e$, in the expected flavor ratio $\nu_\mu : \nu_e = 2 : 1$ for both neutrinos and antineutrinos. Here we focus on $\nu_\mu, \bar{\nu}_\mu$, for which detectors are the most sensitive. The fluxes of γ and $\nu_\mu + \bar{\nu}_\mu$ are shown in Fig. 2, for $k = 2.1$. They are compared to the flux of atmospheric ν_μ, which constitutes the main background. For this, we used the model in [19], extrapolated to fit the high energy IceCube data [16]. At our energies of interest, flavor oscillations are negligible for atmospheric neutrinos, due to the short propagation length. However, they are effective for the FB flux, so that the ν_μ flux at Earth is about 1/2 of the unoscillated one (see e.g. [20]).

Let us comment on the energetics of the CA model. The total number of γ-ray producing cosmic-ray protons, in steady state, in the FB is $\int dE \, N_p(E) \approx$
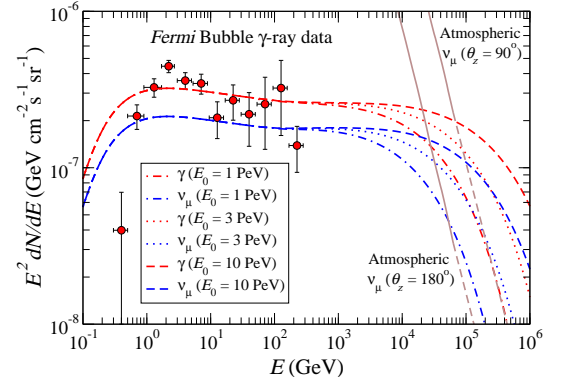

FIG. 2: The fluxes of γ and of ν_μ (total of neutrinos and antineutrinos) from the FB, for different proton cutoff energy E_0 (Eq. (1)), compared with the atmospheric ν_μ flux and the *Fermi*-LAT data [3]. Errors are 1σ.

4.3×10^{57} $(\langle n_H \rangle/10^{-2}$ cm$^{-3})^{-1}(D/8.5$ kpc$)^2$, where $D = 8.5$ kpc is the distance to the bubble centers [3]. The total energy in steady state cosmic-ray proton population is $\int dE \, N_p(E)E \approx 5.4 \times 10^{55}$ $(\langle n_H \rangle/10^{-2}$ cm$^{-3})^{-1}(D/8.5$ kpc$)^2$ ergs. For comparison, with a 2×10^{37} erg s^{-1} power in γ rays from both bubbles [26] and a $\sim 5 \times 10^9$ yr lifetime of the FB, the total energy emitted in γ rays is $\sim 3 \times 10^{54}$ ergs. This is $\sim 6\%$ of the total cosmic-ray proton energy, an efficiency typical of hadronic models.

In order to produce the observed uniform surface brightness of FB, a volume emissivity of the form $(R^2 - r^2)^{-1/2}; (r < R \approx 3.5$ kpc$)$ seems required [3]. Whether this can in principle be obtained in the hadronic scenario has not been studied and is beyond our purpose here. A possibility is that anisotropies can arise from the diffusion of cosmic rays in the magnetic field generated by the shocked shells of the bubble [27]. In any case, the ν flux should trace the γ-ray flux from the FB, and therefore have the same uniform projected intensity.

Under this assumption, we can write the number of ν_μ events accumulated in a certain exposure time t_{exp}, and from a certain zenith bin $[\theta_1, \theta_2]$, (with respect to the detector's position) as follows:

$$N_\nu = \int_0^{t_{exp}} dt \int_{\substack{\Sigma(t) \\ \theta_1 \leq \theta_z \leq \theta_2}} d\Omega \int_{E_{th}}^{\infty} dE \Phi(E) A_\nu(E, \theta_z)$$

$$\simeq t_{exp} \langle \Omega(\theta_1, \theta_2) \rangle_t \int_{E_{th}}^{\infty} dE \Phi(E) \langle A_\nu(E) \rangle_\theta , \quad (3)$$

with a completely analogous expression for $\bar{\nu}_\mu$. Here A_ν is the detector's effective area, θ_z is the zenith angle with respect to the detector, and $\Sigma(t)$ indicates that the integral in the solid angle is done over the region of the bubbles for which the condition on the zenith angle is satisfied. This region depends on the time of the day, due to the revolution of the Earth (Fig. 1). The approximation in Eq. (3) uses the time-averaged solid angle, $\langle \Omega(\theta_1, \theta_2) \rangle_t$,

and the effective area averaged over the zenith bin of interest, $\langle A_\nu(E)\rangle_\theta$. The latter is adequate for sufficiently narrow bins, since A_ν varies gently with θ_z.

As a benchmark, we use twice the effective area of the IC40 configuration of IceCube [16], $A_\nu = 2A_{\mathrm{IC40}}$, which well represents the full IceCube configuration [21] and is reasonable for KM3NeT. We take a 10-year exposure, and consider only the $\nu_\mu + \bar{\nu}_\mu$ flux in sub-horizon directions, $\theta_z > 90°$, as these channels dominate the effective area.

Under this condition, a detector in the northern hemisphere is more sensitive to the FB compared to a southern one since the Galactic center is in the southern hemisphere (Fig. 1). This appears clearly in Fig. 3, which shows the ratio $\langle\Omega(\theta_1,\theta_2)\rangle_t/\Omega_b$, for different zenith bins of interest, and as a function of the detector's latitude, θ_{lat}. IceCube, at $\theta_{lat} = -90°$, is sensitive only to the small portion of the upper bubble that lies in the northern hemisphere (Fig. 1), for which $\langle\Omega\rangle_t \approx 0.02$ sr. For KM3NeT we used $\theta_{lat} = +43°$, the position of the current ANTARES detector in the Mediterranean [22], and we have a much more encouraging total of $\langle\Omega(\cos\theta_z < 0)\rangle_t \approx 0.57$ sr (Fig. 3). Note that this location is nearly optimal (maximum solid angle) for events in the deepest bin, $\cos\theta_z < -0.66$, where the signal to background ratio is the highest (see below). This bin corresponds to a cone of opening angle $\sim 48°$, which is wide enough to contain both bubbles almost completely when the center of the lower bubble is at $\theta_z \sim 180°$ from the detector (Fig. 1).
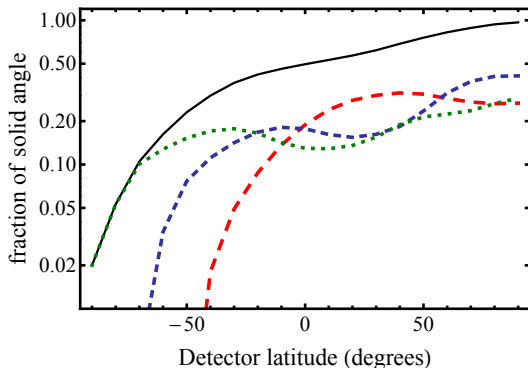

FIG. 3: Daily-average fraction of the solid angle subtended by the *Fermi* bubbles, $\Omega_b = 0.808$ sr, that falls in a given bin of zenith angle, θ_z (with respect to the detector), as a function of the detector latitude. The bins in $\cos\theta_z$ are: $[-1, -0.66]$ (long dashed), $[-0.66, -0.33]$ (short dashed), $[-0.33, 0]$ (dotted) and [-1,0] (total sub-horizon, solid).

Figure 4 (top panel) shows the number of signal and background events at KM3NeT, as a function of E_{th} for the entire region of sensitivity ($\cos\theta_z < 0$) and for the deepest zenith bin ($\cos\theta_z < -0.66$). They are in rough agreement with the earlier estimates in [7].

Counting on the good directional sensitivity of the detector, we restrict the analysis of the background to the daily-averaged solid angles subtended by the bubbles, for better signal discrimination. For the entire sub-horizon solid angle (solid line in fig. 3), and for $E_0 = 3, 10$ PeV, the signal exceeds the background above $\sim 50 - 100$ TeV, where $\sim 20 - 100$ signal events are expected. We found that $E_{th} \sim 20 - 30$ TeV gives the maximum statistical excess of the signal over the background, $\Delta = N_{sig}/\sqrt{N_{sig} + N_{bkg}}$, which is between 4 and 6 σ (i.e., $\Delta \sim 4 - 6$).

For the deepest zenith bin the event rate falls faster with E_{th}, compared to the entire region of zenith, reflecting the stronger opacity of the Earth to ν's crossing its diameter. However the atmospheric flux is also suppressed due to the strongest absorption of muons. Therefore the signal is higher than background already above ~ 20 TeV in the most optimistic case. The statistical significance of the signal is lower due to the lower number of events, but it exceeds 3σ for $E_0 = 3, 10$ PeV, nevertheless.

The zenith distributions of the signal and background are given in Fig. 4 (bottom panel), together with the quantity $\sqrt{N_{sig} + N_{bkg}}$ in the form of error bars. In all cases, the numbers of signal events in the three bins are similar. This is because the strongest neutrino absorption in the deepest bin (lower A_ν) compensates for the larger solid angle. The figure also confirms how the number of events in the deepest bin and in the total sub-horizon region are the best indicators of the effect, in terms of statistical significance, while the other two bins individually suffer from low statistics and high background.

Some remarks are in order. We have taken $k = 2.1$, but results obtained with a much more conservative cosmic-ray proton spectrum, $k = 2.3$, also fit the γ-ray data [7]. In this case, the ν event rate is dominated by background, and $\Delta \sim 1.2\sqrt{t_{exp}/10 \text{ yr}}$, for $\cos\theta_z < 0$. A ~ 6 times longer exposure would be required to reach 3σ. Note, however, that using $\Delta > 3$ as criterion of statistical significance is conservative. Indeed, an excess below 3σ in number of events is likely to be further substantiated, in a full fit of the data, by other indicators like the correlation with the position and extent of the FB.

Briefly, let us comment on the sensitivity of a south pole detector. Due to the suppression in the solid angle and the near-horizon direction of the signal, the number of signal events is low and the background level is enhanced compared to KM3NeT. For the best case scenario of $E_0 = 10$ PeV, we find $N_{sig} = 8.0$ and $N_{bkg} = 59$ for $E_{th} = 10$ TeV, and $N_{sig} = 2.4$ and $N_{bkg} = 1.7$ for $E_{th} = 100$ TeV. Thus, an excess above background will not be statistically significant, unless an exposure at least ~ 6–9 times larger is achieved or efforts to gain sensitivity to events above the horizon [23] and to better discriminate background (e.g., by detecting tau neutrinos [24]) are successful. While a discovery with IceCube seems unlikely, still an analysis of the IceCube data might place interesting constraints on the parameters: for example, it may be able to exclude larger, less natural, values of E_0 or harder proton spectra, $k < 2.1$.
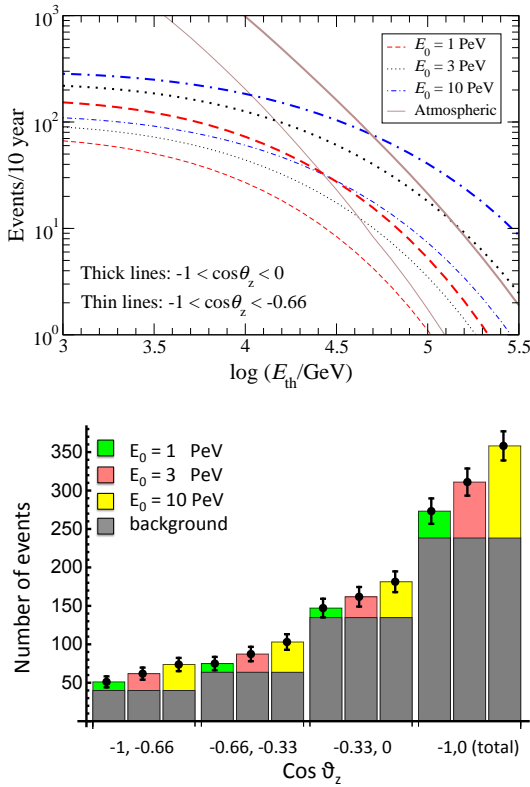
FIG. 4: Number of signal and background events in 10 years, at a km scale detector at $+43°$ latitude, for different cutoff energy E_0 in the proton spectrum. Top: as a function of the energy threshold, E_{th}. Bottom: zenith distribution, for $E_{th} = 25$ TeV. Expected 1σ error bars are shown.

In summary, the FB are a potential new source of galactic high energy neutrinos. For spectral cutoff $E_0 \sim$ 1–10 PeV, and spectral index $k \sim 2.1$ for cosmic-ray protons – motivated by particle acceleration in SNRs – the neutrino flux could exceed the atmospheric background above $\sim 20 - 50$ TeV and be seen at km-scale detectors. For a steeper spectrum, detection will require longer exposures or larger detectors. IceCube is strongly disadvantaged by its southern location, but it could obtain important constraints, and might achieve detection with an increased sensitivity to the sky above the horizon. Our results motivate efforts in this direction. For a northern detector, observing the FB with a decade of operation is a realistic goal, that contributes to make the case for the planned KM3NeT in the Mediterranean. It is encouraging that the Italian node of KM3NeT is funded [25].

The observation of neutrinos from the FB would strongly support the hadronic origin of γ rays from these mysterious objects and favor the model for $\sim 10^9$ years scale activity at the Galactic center to form the FB [7]. The shape of the neutrino spectrum would help to distinguish this scenario from more exotic neutrino-emitting explanations of the FB, like dark matter annihilation or decay [6]. A null result would indicate a softer proton spectra or a non-hadronic mechanism as a primary origin of γ rays and favor $\sim 10^6$ years scale activity by Sgr A* to form the FB [3].

As neutrino and γ-ray detectors progress, it is likely that their interplay will ultimately identify the nature and origin of the FB. Implications will be far reaching, showing what high energy phenomena are at play in our galaxy and, by extension, in other galaxies too.

[*] Electronic address: Cecilia.Lunardini@asu.edu
[†] Electronic address: srazzaqu@gmu.edu
[1] W. B. Atwood *et al.*, Astrophys. J. **697**, 1071 (2009).
[2] G. Dobler *et al.*, Astrophys. J. **717**, 825 (2010).
[3] M. Su, T. R. Slatyer and D. P. Finkbeiner, Astrophys. J. **724**, 1044 (2010).
[4] D. P. Finkbeiner, Astrophys. J. **614**, 186 (2004).
[5] S. L. Snowden *et al.*, Astrophys. J. **485**, 125 (1997).
[6] D. Malyshev, I. Cholis and J. D. Gelfand, Astrophys. J. **722**, 1939 (2010).
[7] R. M. Crocker and F. Aharonian, Phys. Rev. Lett. **106**, 101102 (2011).
[8] P. Mertsch and S. Sarkar, Phys. Rev. Lett. **107**, 091101 (2011).
[9] K. S. Cheng *et al.*, arXiv:1103.1002.
[10] K. Zubovas, A. R. King and S. Nayakshin, Mon. Not. R. Astron. Soc. 415, L21 - L25 (2011).
[11] F. Vissani and F. Aharonian, arXiv:1112.3911.
[12] F. W. Stecker, Astrophys. J. **228**, 919 (1979).
[13] http://icecube.wisc.edu/
[14] http://www.km3net.org/home.php
[15] R. Abbasi *et al.*, arXiv:1109.6096.
[16] R. Abbasi *et al.*, Phys. Rev. D **83**, 012001 (2011).
[17] G. Morlino, E. Amato and P. Blasi, Mon. Not. Roy. Astron. Soc. **392**, 240 (2009); D. C. Ellison *et al.*, Astrophys. J. **712**, 287 (2010); V. S. Ptuskin, V. N. Zirakashvili and E. S. Seo, Astrophys. J. **718**, 31 (2010).
[18] S. R. Kelner, F. A. Aharonian and V. V. Bugayov, Phys. Rev. D **74**, 034018 (2006) [Erratum-ibid. D **79**, 039901 (2009)].
[19] M. Honda *et al.*, Phys. Rev. D **52**, 4985 (1995).
[20] M. L. Costantini and F. Vissani, Astropart. Phys. **23**, 477 (2005).
[21] T. Montaruli at Nusky 2011, Trieste, Italy. http://users.ictp.it/~smr2246/
[22] M. Ageron et al., Nucl. Instrum. Meth. A **656**, 11 (2011).
[23] R. Abbasi *et al.*, Phys. Rev. Lett. **103**, 221102 (2009).
[24] D. F. Cowen, J. Phys. Conf. Ser., **60**, 227-230 (2007).
[25] See news on http://www.lns.infn.it
[26] The power is overestimated by a factor 2 in [3], M. Su, priv. commun.
[27] R. Crocker, priv. commun.